TRG INC.

[redacted]

TECHNICAL RESEARCH GROUP
2 AERIAL WAY · SYOSSET, N. Y.

2676

NYO-~~2674~~
TRG-129-QTR-4

HETEROGENEOUS REACTOR CALCULATION METHODS

Carl N. Klahr
Lawrence B. Mendelsohn

Quarterly Progress Report No. 4 [FOUR]

Jan. 1 - March 31, 1960
AEC Contract No. AT(30-1) - 2375

Submitted to:

U. S. Atomic Energy Commission
Washington, D. C.

Submitted by:

TRG, Incorporated
2 Aerial Way
Syosset, New York

Authors:

Carl N. Klahr

Lawrence B. Mendelsohn

Department Head:

Raphael Thompson

282 1

HETEROGENEOUS REACTOR CALCULATION METHODS

Quarterly Progress Report No.4

Carl N, Klahr
Lawrence B. Mendelsohn

TECHNICAL RESEARCH GROUP

TABLE OF CONTENTS

Section 1. Introduction

This report presents progress in three areas in bringing the heterogeneous reactor calculation method[1] to the point where it will be a useful tool for reactor physics and design, and a more accurate method of analyses than the conventional homogenized methods for a number of important problems. The three areas are: (1) multiple fission and absorption resonance effects, which adapt heterogeneous methods to reactors with any spectrum of fissions; (2) a critical appraisal of the heterogeneous parameters, and a better physical understanding of their values; (3) the acquisition of HERESY 1 calculating experience on D_2O lattices, equivalent to our previous experience with graphite moderated systems.[2]

A set of heterogeneous equations has been formulated that will include epithermal fission and resonance absorption at an arbitrary number of resonances. These equations have been expressed in terms of type-to-type matrices, thus permitting analysis of configurations with a large (of the order of thousands) number of rods. An iterative procedure has been formulated to solve these equations in such a way that the number of independent equations is equal to the number of rod types. Previous results seemed to require a much larger number of equations in the rigorous formulation.[3]

This set of heterogeneous equations will be set up and solved in the HERESY 2 code which will treat multiple fission and absorption resonances. Much of the programming and coding for HERESY 2 has been completed. The inclusion of multiple resonance effects will bring the level of sophistication of the treatment of the energy spectrum at least up to a par with conventional methods while maintaining the advantages of heterogeneous calculations in the spatial treatment. Indeed, it is shown in this report that the multiple resonance formalism permits calculation of fast, intermediate, and epithermal reactors. The problem of calculating the slowing down density at any resonance is rigorously solved in an appendix in terms of type-to-type matrices. The general plan of HERESY 2 is described.

A start has been made on the assembly and use of epithermal fission resonance data in the form of heterogeneous parameters. One result of our program will be to identify important experimental data that is necessary. A discussion of the multiple resonance treatment and related topics is given in Section 2 and in Appendix II.

A critical analysis of the assumptions of the heterogeneous method has been made, in connection with the evaluation of the parameters γ (for thermal absorption) and A (for the single equivalent resonance absorption) which are used in HERESY 1. It is shown that the calculation results are consistent with the assumption that both γ and A are properties of a single rod[4] and

of the moderator, and are independent of the core configuration within a wide range of lattice spacings. The concepts of the asymptotic flux and the self-consistent method on which our method of obtaining the heterogeneous parameters are based, seem therefore, to be quite useful. A physical understanding has been obtained of the variation of γ with the rod size and the moderator, and of the variation of A with the moderator.

This analysis seems to point to a closer examination of the rod-to-rod kernel as a requisite for a better understanding of heterogeneous calculations.

The considerations above are discussed in Section 3.

Another important area has been that of obtaining experience in calculating D_2O lattices on the HERESY 1 code. Most of the problems which were previously studied for a graphite moderator have been reconsidered for D_2O. In particular, the problems of infinite complex lattices were studied, the approach to criticality of a square lattice, and the analysis of spiked cores in D_2O were examined. No surprises were found. These results are reported in Section 4.

A series of HERESY 1 calculations in a graphite moderator was also carried out to examine the differences between square lattice and hexagonal lattice configurations. Earlier workers[5] have pointed out that hexagonal lattices are somewhat more difficult to study analytically, and it was felt that for equal fuel to moderator volume ratios there might be different results

for the two core patterns. Our studies showed that for a number of equivalent lattices, in the sense of equal fuel to moderator volume ratios, the reactivity and power pattern results are fairly close for square and hexagonal arrays. These results are given in Section 5.

Section 2. Heterogeneous Calculations Including Epithermal Fission

When the nuclear fuel is enriched uranium it may be important to include epithermal fissions in heterogeneous calculations. This is certainly imperative in intermediate and fast reactors. Even in reactors whose spectrum of fissions is predominantly thermal one may have an appreciable fraction of the fissions occurring at non-thermal energies, depending on the enrichment and the lattice spacing. It has been estimated that the effects of epithermal fissions in water moderated reactors may be of the order of 5% in the reactivity.[6]

Physically, the difference between a barn of fission cross section at epithermal versus thermal energies is as follows: Epithermal fission gives the neutron less chance to leak from the reactor, and there is less competition with parasitic absorbers than at thermal, both factors tending to increase the reactivity. On the negative side the value of η is usually less than at thermal since α is larger. The net effect may be to increase or decrease the reactivity. Homogeneous calculations for thermal reactors usually introduce a five factor formula to include epithermal fission

$$k_\infty = \eta \epsilon p f \beta \qquad (2.1)$$

where β is the epithermal fission factor. Arnold[7] gives the following expression for β.

$$\beta = \frac{P_{25}}{1-\epsilon\, p_n N_L \eta_R (1-P_{25})} \qquad (2.2)$$

where P_{25} = overall U^{235} resonance escape probability

p_n = escape probability for resonances above those of U^{235}

N_L = non-leakage probability for energies above U^{235} resonances

η_R = neutrons released per neutron absorbed in U^{235} resonances.

The leakage effect of epithermal fissions can only be included by classifying the epithermal range into one or more energy groups, distinct from the thermal group and calculating the leakage by conventional means.

The question arises, how best to treat epithermal fissions in heterogeneous calculations. A simple minded way would be to lump the factor β in equation (2.1) with η, just as we lump ϵ with η. If this is done one can include epithermal fission effects in the HERESY 1 code. This procedure seems quite arbitrary, however, especially when fuel elements of varying enrichment are present. It is important therefore to calculate both the reactivity and the power distribution in a way that takes the heterogeneous nature of the core into account.

A basic set of heterogeneous equations that include resonance fission effects has been given in the first report of this series.[8] There it was shown that if N rod types are present and if R epithermal fission resonance levels are considered,

the total number of simultaneous equations is N(R+1). This number of equations is unmanageable. However, we have been able to simplify the basic set to number only N. This makes it possible to treat epithermal fissions exactly within a set of only N simultaneous linear equations, where N is the number of rod types. This derivation and the result will be given in this section.

It should be emphasized that the application of the homogeneous equations including resonance fission is not limited to thermal reactors. This set of equations can be applied equally well to any spectrum of fissions - intermediate reactors, fast reactors, or reactors with an arbitrary fraction of the fissions taking place at thermal energies.

We shall formulate the heterogeneous equations including epithermal fission in the simplified matrix notation introduced in the last two reports of this series. Before doing this, however, we shall summarize the system of equations used in HERESY 1, which applies to thermal reactors, to contrast this system with the more general heterogeneous formulation that includes epithermal fissions.

HERESY 1 includes one equivalent absorption resonance and no fission resonance. The heterogeneous equations take the following form:

$$\underline{\underline{\gamma}}\ \underline{i} = \frac{1}{k}\,\underline{\underline{G}} \cdot \underline{i} - \underline{\underline{Z}} \cdot \underline{i} \qquad (2.3)$$

where

$$\underline{\underline{G}} = (\underline{\underline{T}} - \underline{\underline{T}}^{r}\underline{\underline{A}}^{r}\underline{\underline{S}}^{r}) \cdot \underline{\underline{\eta}} \qquad (2.4)$$

These matrices have been defined in previous reports. The definitions are repeated in Appendix I.

If HERESY I were expanded to include many absorption resonances equation (2.3) would stand unchanged but $\underline{\underline{G}}$ would be corrected as follows:

$$\underline{\underline{G}} = (\underline{\underline{T}} - \sum_r \underline{\underline{T}}^r \underline{\underline{A}}^r \underline{\underline{S}}^r)\ \underline{\underline{\eta}} \qquad (2.4A)$$

The summation is taken over the individual absorption resonances, each characterized by a matrix $\underline{\underline{A}}^r$ of resonance A factors for each rod type, and $\underline{\underline{S}}^r$ and $\underline{\underline{T}}^r$ matrices, denoting respectively the type-to-type kernel summations describing slowing down to the r-th resonance and slowing down from the r-th resonance followed by thermal diffusion.

The input data for HERESY I, in addition to the kernel functions, are the $\underline{\underline{\gamma}}$, $\underline{\underline{\eta}}$ and $\underline{\underline{A}}^r$ (for the single equivalent resonance) matrices. The input data with many absorption resonances would be $\underline{\underline{\gamma}}$, $\underline{\underline{\eta}}$ and all the $\underline{\underline{A}}^r$ matrices -- one for each resonance. In addition, kernels to calculate all the $\underline{\underline{T}}^r$ and $\underline{\underline{S}}^r$ matrices would be necessary, instead of just one set of resonance kernels.

Section 2.1 Basic Heterogeneous Equations

When resonance fission is included one wishes to obtain not only the vector $\underline{i}$ of relative thermal absorptions in the individual rod types, but also the vectors $\underline{i}_r$, one for each fission resonance, of relative absorptions in the individual rod types at the r-th fission resonance. The basic heterogeneous equations take the following form in matrix notation when epithermal fissions are included:

$$\underline{\gamma}\, \underline{i} = \frac{1}{k}\, \underline{\underline{G}} \cdot \underline{i} - \underline{\underline{Z}} \cdot \underline{i} + \frac{1}{k} \sum_r \underline{\underline{G}}^r \cdot \underline{i}_r \tag{2.5}$$

$$\underline{i}_r = \frac{1}{k}\, \underline{\underline{A}}^r \cdot \underline{\underline{S}}^r \cdot \underline{\underline{\eta}} \cdot \underline{i} + \frac{1}{k}\, \underline{\underline{A}}^r \cdot \underline{\underline{S}}^r \cdot \left(\sum_P \underline{\underline{\eta}}^P \cdot \underline{i}_P\right) \tag{2.6}$$

where

$$\underline{\underline{G}}^r = \left(\underline{\underline{T}} - \sum_P \underline{\underline{T}}^P\, \underline{\underline{A}}^P\, \underline{\underline{S}}^P\right) \cdot \underline{\underline{\eta}}^r \tag{2.7}$$

The only distinction between absorption resonances and fission resonances in these equations is that $\underline{\underline{\eta}}^r$ is a zero matrix for pure absorption resonances. These equations are simply a rewrite in matrix notation of equations(2.5) and (2.6) of the first report[8] in this series in terms of type-to-type matrix elements. Recursion relations to calculate the matrices $\underline{\underline{S}}^r$ and $\underline{\underline{T}}^r$ are presented in Appendix II.

We shall assume that the following data are available.

a) The matrices $\underline{\underline{\eta}}^r$, $\underline{\underline{A}}^r$, $\underline{\underline{S}}^r$ and $\underline{\underline{T}}^r$ for U^{235} resonances

b) The matrices $\underline{\underline{A}}^r$, $\underline{\underline{S}}^r$, and $\underline{\underline{T}}^r$ for U^{238} resonances

c) A first guess k_o for the reactivity of the configuration.

We shall define

$$\underline{\underline{Q}} = \underline{\underline{T}} - \Sigma\, \underline{\underline{T}}^P\, \underline{\underline{A}}^P\, \underline{\underline{S}}^P \tag{2.8}$$

In terms of Q,

$$\underline{\underline{G}} = \underline{\underline{Q}} \cdot \underline{\underline{\eta}} \text{ and } \underline{\underline{G}}^r = \underline{\underline{Q}} \cdot \underline{\underline{\eta}}^r \tag{2.8a}$$

Equations (2.5) and (2.6) can be rewritten as follows in terms of $\underline{\underline{Q}}$:

$$\underline{\gamma}\, \underline{i} = \frac{1}{k}\, \underline{\underline{Q}} \cdot \underline{\underline{\eta}} \cdot \underline{i} - Z\, \underline{i} + \frac{1}{k}\, \underline{\underline{Q}} \cdot \left(\sum_r \underline{\underline{\eta}}^r \cdot \underline{i}_r\right) \tag{2.5a}$$

$$\underline{i}_r = \frac{1}{k}\, \underline{\underline{A}}^r \cdot \underline{\underline{S}}^r \cdot \underline{\underline{\eta}}\, \underline{i} + \frac{1}{k}\, \underline{\underline{A}}^r \cdot \underline{\underline{S}}^r \cdot \left(\sum_P \underline{\underline{\eta}}^P \cdot \underline{i}_P\right) \tag{2.6a}$$

where $\underline{\underline{\eta}}$ is the matrix of neutron yield per fuel absorption for thermal absorptions in the fuel.

From (2.6a) we can calculate the quantity $\left(\sum_r \underline{\underline{\eta}}^r \cdot \underline{i}_r\right)$. One obtains

$$\left(\sum_P \underline{\underline{\eta}}^P \cdot \underline{i}_P\right) = \left[1 - \frac{1}{k} \sum_r \underline{\underline{\eta}}^r \cdot \underline{\underline{A}}^r \cdot \underline{\underline{S}}^r\right]^{-1} \cdot \frac{1}{k} \sum_r \underline{\underline{\eta}}^r \cdot \underline{\underline{A}}^r \cdot \underline{\underline{S}}^r \cdot \underline{\underline{\eta}} \cdot \underline{i} \tag{2.9}$$

We shall define the matrix $\underline{\underline{\alpha}}$

$$\underline{\underline{\alpha}} = \frac{1}{k} \sum_r \underline{\underline{\eta}}^r \cdot \underline{\underline{A}}^r \cdot \underline{\underline{S}}^r \tag{2.10}$$

Substituting (2.9) into (2.5a) one obtains

$$\underline{\gamma}\,\underline{i} = \frac{1}{k}\,\underline{Q}\cdot\left[1 - \underline{\underline{\alpha}}\right]^{-1}\cdot\underline{\underline{\eta}}\cdot\underline{i} - \underline{\underline{Z}}\cdot\underline{i} \tag{2.11}$$

If one defines $$\underline{\underline{N}} = \left[1 - \underline{\underline{\alpha}}\right]^{-1}\cdot\underline{\underline{\eta}} \tag{2.12}$$

equation (2.11) takes the form

$$\underline{\gamma}\cdot\underline{i} = \frac{1}{k}\,\underline{Q}\cdot\underline{N}\cdot\underline{i} - \underline{Z}\,\underline{i} \tag{2.13}$$

This equation has the same form as equation (2.3) which is solved in the HERESY 1 code.[9] The principal difference is that $\underline{Q}$ includes absorption effects of many resonances and that $\underline{\underline{N}}$ replaces $\underline{\underline{\eta}}$. $\underline{\underline{\eta}}$ is a diagonal matrix referring to thermal fissions. $\underline{\underline{N}}$ is a non-diagonal matrix referring to both thermal and non-thermal fissions.

The vector of resonance absorption $\underline{i}_r$ is given by

$$i_r = \frac{1}{k}\,\underline{\underline{A}}^r\cdot\underline{\underline{S}}^r\cdot\underline{\underline{N}}\cdot\underline{i} \tag{2.14}$$

Equations (2.10), (2.12), (2.13) and (2.14) lead to a simple procedure for solving the heterogeneous equations (2.5) and (2.6) for any reactor, regardless of the spectrum of fissions. If neutron absorptions occur at R epithermal energy intervals (or at R resonance levels) and at thermal energies this is equivalent to R + 1 energy groups. First we shall assume that thermal fissions are significant. The procedure is then as follows:

(1) An initial guess of the reactivity, k_o, is assumed

(2) One calculates the matrix α from (2.10) and then $\underline{\underline{N}}$ from (2.12) using this initial guess

(3) Equation (2.13) is solved for the reactivity k and the vector of thermal absorptions

(4) Equation (2.14) is then solved for $\underline{i}_r$ corresponding to the computed k.

(5) If k calculated in step (3) agrees with the initial guess k_o, to within some predetermined error limit, the calculation is completed. If the difference $k-k_o$ is significant, one takes a new guess for k and proceeds to step (2) again

(6) The iteration process is continued until k calculated from equation (2.13) agrees with the last guess of k. The $\underline{i}$ and $\underline{i}_r$ vectors yield the pattern of absorptions

(7) The power distribution $\underline{P}$ among the rod types is given by

$$\underline{P} = \underline{\underline{W}}\, \underline{i} + \Sigma\, \underline{\underline{W}}^r\, \underline{i}_r \qquad (2.15)$$

The $\underline{\underline{W}}$'s are diagonal matrices for each resonance and at thermal whose diagonal elements give the fraction of absorptions which result in fission for each rod type.

One should note that the procedure does not require the solution of N . (R + 1) simultaneous equations, where N is the number of rod types, but only of N simultaneous equations. For a

reactor whose fission spectrum is predominantly thermal only one initial guess would probably be required, and this could be obtained from HERESY 1. Alternatively if β is significantly different from 1, an initial guess of β times the result for the thermal reactor can be taken. The initial guess might also come from a conventional homogeneous calculation.

These equations can also be applied to non-thermal reactors. It is convenient to choose thermal energy as a reference if a large fraction of the fissions occur there. Otherwise, any energy level can be chosen as the reference. The unique feature of thermal neutrons is the presence of a $\underline{\underline{Z}}$ matrix denoting diffusion without energy loss. If no fissions occurred at thermal energy all the equations would have the form

$$\underline{i}_r = \frac{1}{k} \underline{\underline{A}}^r \cdot \underline{\underline{S}}^r \cdot \left(\sum_P \underline{\underline{\eta}}^P \, i_P \right) \tag{2.16}$$

One could choose any resonance energy r=b and arbitrarily use absorptions in this energy interval as the reference vector $\underline{i}_b$. If a large fraction of the fissions occurred at this reference energy b the convergence properties of the procedure would be rapid, although the procedure would converge in any case. We rewrite (2.16) in terms of the reference vector $\underline{i}_b$

$$\underline{i}_b = \frac{1}{k} \underline{\underline{A}}^b \cdot \underline{\underline{S}}^b \cdot \underline{\underline{\eta}}^b \cdot \underline{i}_b + \frac{1}{k} \underline{\underline{A}}^b \cdot \underline{\underline{S}}^b \cdot \left(\sum_P{}' \underline{\underline{\eta}}^P \cdot \underline{i}_P \right) \tag{2.17}$$

$$\underline{i}_r = \frac{1}{k} \underline{\underline{A}}^r \cdot \underline{\underline{S}}^r \cdot \underline{\underline{\eta}}^b \cdot \underline{i}_b + \frac{1}{k} \underline{\underline{A}}^r \cdot \underline{\underline{S}}^r \cdot \left(\sum_P{}' \underline{\underline{\eta}}^P \cdot \underline{i}_P \right) \tag{2.18}$$

The prime in the sum over resonances denotes that the reference level b is not included in the sum. Equations (2.17) and the set of R-1 equations denoted by (2.18) are analogous to (2.5a) and (2.6a).

Again the solution hinges on defining matrices $\underline{\underline{\alpha}}'$ and $\underline{\underline{N}}'$

$$\alpha' = \frac{1}{k} \sum_{P}{}' \underline{\underline{\eta}}^{P} \cdot \underline{\underline{A}}^{P} \cdot \underline{\underline{S}}^{P} \tag{2.19}$$

$$N = \left[1 - \underline{\underline{\alpha}}'\right]^{-1} \cdot \underline{\underline{\eta}}^{b} \tag{2.20}$$

whereupon equation (2.17) becomes

$$i_b = \frac{1}{k} \underline{\underline{A}}^{b} \cdot \underline{\underline{S}}^{b} \cdot \underline{\underline{N}}' \cdot \underline{i}_b \tag{2.17a}$$

This equation can be solved by iteration as before. When the $\underline{i}_b$ vector and k have been obtained, the resonance vectors i_r can be obtained as follows:

$$i_r = \frac{1}{k} \underline{\underline{A}}^{r} \cdot \underline{\underline{S}}^{r} \cdot \underline{\underline{N}}' \cdot \underline{i}_b \tag{2.18a}$$

It is clear from this procedure which does not choose any preferential energy level or any energy interval that this procedure is the heterogeneous analogue of a many group treatment. It can be used to calculate fast, intermediate, or mixed spectrum reactors. The $\underline{\underline{S}}^{r}$ matrices, which describe the slowing down process, are calculated according to the procedure given in Appendix II.

The interpretation of the $\underline{\alpha}$ matrix is as follows. α_{nm} is the number of resonance fission neutrons born at rod type n due

to a fission neutron emitted at rod type m. Let ψ_n be the total number of fission neutrons born at rod type n. Then

$$\sum_m \alpha_{nm} \psi_m < \psi_n \tag{2.21}$$

or

$$\underline{\underline{\alpha}} \ \underline{\psi} < \underline{\psi} \tag{2.21a}$$

The reason for the inequality is that all fissions are not resonance fissions. In the case of a thermal reactor this is because thermal fissions also contribute. When energy level b is the reference energy the inequality holds because the reference level is not counted among the other resonance levels that contribute to $\underline{\underline{\alpha}}$. According to (2.21a) the matrix $\underline{\underline{\alpha}}$ has eigenvalues less than unity. Therefore the matrix

$$\left[1 - \underline{\underline{\alpha}}\right]^{-1} = 1 + \underline{\underline{\alpha}} + \underline{\underline{\alpha}}^2 + \underline{\underline{\alpha}}^3 + \ldots \tag{2.22}$$

converges and the procedure is valid. Note that the larger the fraction of fissions at the reference level b (or at thermal) the smaller the eigenvalues of $\underline{\underline{\alpha}}$ will be, and the more rapidly the series (2.22) will converge.

Section 2.2 HERESY 2 Program Description

Work is in progress to produce a heterogeneous physics calculation code that will account for fissions at epithermal energies, and will permit many absorption resonances to be considered. This code has been dubbed HERESY 2. It is important for the following reasons:

1. It will be the analogue of a multi-energy (multi-group) calculation technique for the heterogeneous method, permitting treatment of thermal reactors with substantial epithermal fission, of intermediate reactors, and even of fast reactors, by heterogeneous physics methods.
2. It will permit numerical experimentation to determine the importance of a many resonance treatment vs. a single (or a few) equivalent resonances with regard to their effects on k and on the power pattern. This applies to both absorption resonances and fission resonances.
3. It will permit numerical experimentation to determine the required accuracy of the heterogeneous resonance parameters, in terms of their effects on k and the power pattern. This effort will be useful in determining the scope of future experimental programs to measure heterogeneous resonance parameters.

4. The sensitivity analysis of reasons 2 and 3 will be important not only to provide basic reactor physics data but to point the way to simplified, yet accurate, reactor physics methods and codes.

The equations of HERESY 2 are equations (2.13) and (2.14) which we now repeat

$$\underline{\underline{\gamma}}\,\underline{i} = \frac{1}{k}\,\underline{\underline{Q}}\cdot\underline{\underline{N}}\cdot\underline{i} - \underline{\underline{Z}}\,\underline{i} \qquad (2.13)$$

$$i_r = \frac{1}{k}\,\underline{\underline{A}}^r\cdot\underline{\underline{S}}^r\cdot\underline{\underline{N}}\cdot\underline{i} \qquad r = 1, 2, \ldots R \qquad (2.14)$$

where

$$\underline{\underline{N}} = \left[1 - \underline{\underline{\alpha}}\right]^{-1}\cdot\underline{\underline{\eta}} \qquad (2.12)$$

$$\underline{\underline{\alpha}} = \frac{1}{k}\sum_r \underline{\underline{\eta}}^r\cdot\underline{\underline{A}}^r\cdot\underline{\underline{S}}^r \qquad (2.10)$$

$$\underline{\underline{Q}} = \underline{\underline{T}} - \sum_P \underline{\underline{T}}^P\cdot\underline{\underline{A}}^P\cdot\underline{\underline{S}}^P \qquad (2.8)$$

This set of equations is written in a manner that emphasizes thermal fissions. It is most appropriate for an epithermal reactor with an appreciable fraction (100% to 10%) of fissions taking place at thermal energies. For non-thermal reactors one would replace $\underline{i}$ by $\underline{i}_b$, where b denotes a reference energy, preferentially the energy interval with the largest fraction of fissions (to assure rapidity of convergence.) Then one would make the following substitutions in the HERESY 2 equations given above:

$\underline{i}$ is replaced by $\underline{i}_b$

$\underline{\underline{Z}}$ is replaced by the zero matrix

$\underline{\gamma}$ is replaced by $\left[\underline{\underline{A}}^b\right]^{-1}$

$\underline{Q}$ is replaced by $\underline{\underline{S}}^b$

$\underline{\alpha}$ is replaced by $\underline{\alpha}'$, equation (2.19) with summation over only R-1 resonances

$\underline{\underline{N}}$ is replaced by $\underline{\underline{N}}'$, equation (2.20)

The input to HERESY 2 will be as follows:

(1) Rod-to-rod kernels to calculate the following type-to-type matrices: $\underline{\underline{T}}$, $\underline{\underline{Z}}$ at thermal energy and $\underline{\underline{S}}^r$, $\underline{\underline{T}}^r$ for U^{238} absorption resonances, and $\underline{\underline{S}}^r$, $\underline{\underline{T}}^r$, for U^{235} fission resonances

(2) The matrices $\underline{\underline{\eta}}^r$, $\underline{\underline{A}}^r$ for U^{235} fission resonances and $\underline{\underline{A}}^r$ for U^{238} absorption resonances

(3) The matrices $\underline{\gamma}$ and $\underline{\underline{\eta}}$ for thermal energy.

The matrices $\underline{\underline{S}}^r$ and $\underline{\underline{T}}^r$ for all resonances will be calculated by HERESY 2 from the fundamental kernel functions and the resonance parameters matrices $\underline{\underline{A}}^r$ using the recursion relations of Appendix II. Alternatively, it may be preferable to write a separate code to calculate these matrices and specify them as input for HERESY 2. It is necessary to use magnetic tape storage of the multiple resonance data in HERESY 2 because of the limited internal memory capacity of the IBM-704.

The calculation procedure in HERESY 2 will consist of five major subprograms:

1. Calculation of the matrices S^r and T^r for all resonances and transfer of these matrices to magnetic tape storage
2. Calculation of thermal matrices $\underline{\underline{T}}$, $\underline{\underline{Z}}$ and $\underline{\underline{L}}$ and retention in internal memory
3. Calculation of matrices $\underline{\underline{Q}}$ and $\underline{\underline{\alpha}}_{(1)}$ and $\underline{\underline{N}}_{(1)}$. Calculation of the matrix product $\underline{\underline{A}}^r \cdot \underline{\underline{S}}^r$ and transfer to tape storage
4. Iterative solution of

$$\underline{\underline{L}} \cdot \underline{i} = \frac{1}{k} \underline{\underline{Q}} \cdot \underline{\underline{N}} \cdot \underline{i}$$

for k and $\underline{i}$. If k does not agree with the estimate of k used in $\underline{\underline{\alpha}}$ one calculates

$$\underline{\underline{\alpha}}_{(2)} = \frac{k_1}{k_2} \underline{\underline{\alpha}}_{(1)}$$

$\underline{\underline{N}}$ is also recalculated and a new solution is obtained for the above set of equations. The procedure is iterated until it converges

5. Calculation of $\underline{i}_r$ and subsequent data processing.

We will consider these subprograms in detail

1. Calculation of $\underline{\underline{S}}^r$ and $\underline{\underline{T}}^r$ matrices

These type-to-type matrices will be calculated from the fundamental slowing down kernels $g_{ab}(P \rightarrow q)$ and $F_{ab}(P \rightarrow \text{thermal})$, (P and q designate resonance energies, see Appendix II).

these kernels being specified in tabular form as a function of the distance $|\underline{r}_a - \underline{r}_b|$. $\underline{\underline{S}}^P$ is calculated from the recursion relation (II.4) of Appendix II.

$$\underline{\underline{S}}^{P+1} = \underline{\underline{S}}'(o \to P+1) - \sum_{t=1}^{P} \underline{\underline{S}}'(t \to P+1) \cdot \underline{\underline{A}}^t \cdot \underline{\underline{S}}^t \qquad \text{(II.4)}$$

First, however, the matrices $S'(t \to P+1)$ must be calculated from the $g_{ab}(P \to q)$ function

$$S'_{nm}(P \to q) = \sum_{\beta} g_{n\alpha,m\beta}(P \to q) \qquad \text{(II.5)}$$

$\underline{\underline{T}}^r$ is calculated from the recursion relation (II.8) of Appendix II.

$$\underline{\underline{T}}^r = \underline{\underline{T}}'(r \to R+1) - \sum_{t=r+1}^{R} \underline{\underline{T}}'(t \to R+1) \underline{\underline{A}}^t \underline{\underline{S}}^{t-r}(r \to t) \qquad \text{(II.8)}$$

First the $\underline{\underline{S}}^{t-r}(r \to t)$ matrices must be calculated from (II.4) The matrix $\underline{\underline{T}}'(t \to R+1)$ must be generated from the fundamental kernel $F_{ab}(P \to R+1)$ using a formula analogous to (II.5). Finally $\underline{\underline{T}}^r$ is calculated from (II.8). The matrices A^r, S^r, T^r for r=1,2,...R are then stored on magnetic tape for subsequent use.

2. Calculation of thermal matrices $\underline{\underline{T}}$, $\underline{\underline{Z}}$ and $\underline{\underline{L}}$

This procedure is identical to that followed in HERESY 1. A thermal diffusion kernel $f(|r_a - r_b|)$ is used to generate the $\underline{\underline{T}}$ matrix for the core geometry. The $\underline{\underline{\gamma}}$ matrix is read in and $\underline{\underline{L}} = \underline{\underline{Z}} + \underline{\underline{\gamma}}$ is calculated.

3. Calculation of $\underline{\underline{Q}}$, $\underline{\underline{\alpha}}$, $\underline{\underline{N}}$ and $\underline{\underline{A}}^r . \underline{\underline{S}}^r$

The matrices $\underline{\underline{T}}^r$, $\underline{\underline{A}}^r$, $\underline{\underline{S}}^r$ and $\underline{\underline{\eta}}^r$ are read in successively from the tape for each resonance and the following products computed

$$\underline{\underline{Q}} = \underline{\underline{T}} - \sum_{r=1}^{R} \underline{\underline{T}}^r \underline{\underline{A}}^r \underline{\underline{S}}^r$$

$$\underline{\underline{\alpha}}(n) = \frac{1}{k_n} \sum_{r=1}^{R} \underline{\underline{\eta}}^r \underline{\underline{A}}^r \underline{\underline{S}}^r$$

$$\underline{\underline{N}}(n) = \left[1 - \underline{\underline{\alpha}}(n) \right]^{-1} . \underline{\underline{\eta}}$$

$$\underline{\underline{A}}^r . \underline{\underline{S}}^r$$

where

$$\left[1 - \underline{\underline{\alpha}} \right]^{-1} \approx 1 + \underline{\underline{\alpha}} + \underline{\underline{\alpha}}^2 + \underline{\underline{\alpha}}^3 + \ldots$$

The subscript n denotes the n-th iteration corresponding to the eigenvalue guess $k_{(n)}$.

$\underline{\underline{Q}}$, $\underline{\underline{\alpha}}(n)$ and $\underline{\underline{N}}(n)$ are stored in internal memory. The products $\underline{\underline{A}}^r . \underline{\underline{S}}^r$ are stored on tape for use in subprogram 5.

4. Iterative Solution and 5. Calculation of i_r

This has been discussed in detail in Sections 2.1 and 2.2. The final data processing will be similar to that performed in HERESY 1. In addition, however, $\underline{P}$ of equation (2.15) will be calculated, and such quantities as the breeding ratio may be calculated.

Section 2.3 Resonance Fission Parameters

Resonance fission effects require the specification of a parameter A_n^p at the p-th resonance for the n-th rod, where p is a fission resonance of U^{235}. The most direct way to obtain the individual A_n^p, requires measurement of fission resonance escape probabilities of the individual resonance levels in an infinite lattice. If this probability is P_p in an infinite one component lattice of rods of the type considered, and if the area of the unit cell is σ then[10]

$$P_p = 1 - \frac{A^p}{\sigma} \tag{2.23}$$

Experimental or theoretical determinations of these individual resonance parameters are in short supply. However, one can obtain a single lumped (equivalent) fission resonance parameter from an experimental determination of the thermal utilization(f) and δ_{25} where:

$$\delta_{25} = \frac{\text{fast fissions in } U^{235}}{\text{thermal fissions in } U^{235}} \tag{2.24}$$

$$f = \frac{\text{thermal fissions in } U^{235}}{\text{all thermal absorptions}} \tag{2.25}$$

Substituting (2.24) in (2.25)

$$f\delta_{25} = \frac{\text{fast fissions in } U^{235}}{\text{all thermal absorptions}} \tag{2.26}$$

We want to calculate P_{235} = resonance escape probability in U^{235}

$$P_{235} = \frac{X(\text{Neutrons reaching thermal with } U^{235} \text{ resonance absorption})}{Y(\text{Neutrons reaching thermal with no } U^{235} \text{ resonance absorption})} \tag{2.27}$$

For an infinite lattice, we can neglect thermal leakage. Therefore, all thermal absorptions = X.

Substituting in (2.26) we obtain fast fissions in $U^{235} = f\delta_{25}X$ (2.28)

Thus for the neutrons (Y) reaching thermal with no resonance absorption effects we have:

$$Y = X + f\delta_{25}X \tag{2.29}$$

Substituting (2.29) into (2.27)

$$P_{235} = \frac{1}{1+f\delta_{25}} \tag{2.30}$$

Once P_{235} is obtained, we can find the A_n(lumped) for one equivalent U^{235} fission resonance using (2.23). Thus we obtain the lumped resonance fission parameter

$$A_{235}(\text{lumped}) = \frac{f\delta_{25}\sigma}{1+f\delta_{25}} \tag{2.31}$$

To give some idea of the importance of the resonance fission effect in enriched U-H_2O lattices,[11] we cite

$$A_{235} \approx \frac{1}{2} A_{238}$$

as the result for a close packed system of 1.3% enriched uranium in a water moderator where A_{238} is the parameter for

lumped U^{238} resonance absorption. For a $\frac{\text{Vol } H_2O}{\text{Vol } U} = 1/1$ system, we obtained $A_{235} = .73$ cm^2 using the experimental results cited in (11) for rods of .387" diameter.

We now turn to a more difficult problem -- obtaining a set of A_n^P's for the individual fission resonances of rod n. Direct data seems to be unavailable. However, there are at least two methods that one might suggest for synthesizing a set of A_n^P's to be used for numerical experimentation with the HERESY 2 code (sensitivity analysis).

Method 1: Having obtained the single (lumped) equivalent fission resonance parameter A_{235}, we can assume various reasonable individual resonance fission schemes and determine the sensitivity of the code-output to the assumed schemes. One such scheme might be to break up the interval between 1 and 100 ev into 10 resonances of equal strength, each resonance having an $A^P = \frac{A_{235}^{\text{lumped}}}{10}$.

Method 2: Another approach is to use the cross section data in Reference (12) to compute the integral

$$I_i = \int_{\text{Resonance } i} \frac{\sigma_F(E)\,dE}{E}$$

by an approximate numerical integration technique, where σ_F = fission cross section of U^{235} for each resonance. Then we know that to a fair approximation A_F^P is proportional to I_P. We also

approximate $\sum_P A^P = A_{235}^{\text{lumped}}$. Thus we could determine all the A^P's. The only difficulty is that the available data only allows us to obtain I_i for resonances up to 10.15 ev. We cite the results of the numerical integrations for these lower energy fission resonances in the following table 1. Additional but incomplete information about the resonance fission at higher energies up to 35.3 ev can be found in the cited reference.

Should it turn out that the code has a relatively small sensitivity to the assumed individual resonance pattern, it may not prove worthwhile to perform a more intense investigation to determine the individual A^P's.

It is important to note that experimental results for A_{235} for a given rod in one moderator may be used to estimate A_{235} for an identical rod in another moderator. The considerations of Section 3.3 would be utilized. This can be useful, for example, when experimental data on δ_{235} are available in water and not in graphite. Since fuel rods in graphite will be much thicker than fuel pins in water, it will also be necessary to correct A_{235} for the changed rod size. Hence this method can only give order of magnitude results. For some purposes, however, this can be quite useful.

Table 1

Energy of i-th Resonance (ev)	$I_i = \int_{\text{Resonance } i} \frac{\sigma_F(E)\, dE}{E}$
1.127	46.7
2.04	4.28
2.82	2.02
3.14	5.16
3.61	6.34
4.84	2.27
5.45	1.24
6.12	1.85
6.40	7.53
7.10	2.55
8.82	2.07
9.27	2.68
9.74	.68
10.15	.80

Section 3. Evaluation of γ and A in Various Moderators

In this section we wish to consider and compare typical values of the thermal parameter, γ, and the resonance absorption parameter A for a single equivalent lumped resonance in several moderators. This comparison is important because it involves a critical examination of the basic ideas of the heterogeneous reactor physics method.

Our methods for calculating γ and A involve the asymptotic flux, not the real flux at the rod surface. As a matter of fact, all of our heterogeneous physics theory uses the asymptotic flux and not the real flux. Other workers have not used this approach explicitly. We define the asymptotic flux at the rod in question by extrapolating back to the rod surface the thermal flux in the moderator at distances of a couple of mean free paths and more from the rod. In this way the rod-moderator boundary effects do not affect the asymptotic flux. Perhaps a better definition is the following: we shall conceptually shrink the radial dimensions of each rod to the point where it becomes a delta function in position (line source and sink); meanwhile we assume that the source intensity and sink intensity of each of the rods (including self effects) remain unchanged. The flux calculated from this configuration of delta function rods evaluated at the rod position is called the asymptotic flux in

the moderator at that rod. Thus γ is defined as

$$\gamma = \frac{\text{asymptotic flux at the rod}}{\text{true number of absorptions per sec per unit rod length at that rod}}$$

It should be emphasized that the asymptotic flux at a rod is not necessarily a measureable quantity, and is certainly not equal to the flux at the rod surface.

Our methods for calculating γ and A also involve the self-consistent method. This method calculates γ or A in a one-component infinite lattice of rods of the type considered using measured values (or calculated values based on some acceptable recipe) of the thermal utilization, in the case of γ, or of the resonance escape probability in the case of A. One uses the same set of kernels in calculating γ or A that one will later use with the values of γ or A which are derived. By choosing γ or A to fit an experimentally determined f or p one makes it capable of generating realistic reactor physics despite its use with the asymptotic flux rather than the real flux.

The use of the asymptotic flux and the determination of γ and A by the self-consistent method provide a simple and seemingly accurate heterogeneous procedure. If one had to calculate the real flux at the rod surface the procedure would be much more difficult. Using the asymptotic flux does not seem to impair the accuracy of the calculations. It appears that the boundary effect error in the asymptotic flux value is canceled out, so to speak, by the self-consistent procedure.

The asymptotic flux and the self-consistent method also counter two objections that one would raise against heterogeneous reactor physics calculations. There are four major objections that one can bring up.

1. The finite size of a rod. This makes the "flux at a rod" non-unique since it can vary considerably around the rod. It also introduces the rod-moderator boundary effects.
2. The angular distribution of the flux at a rod is not known, hence the absorptions are difficult to calculate.
3. Displacement of moderator by fuel makes the infinite moderator model used in heterogeneous calculations incorrect.
4. Correct slowing down and diffusion kernels are required to distribute the flux from a source correctly among the various rods.

Use of the asymptotic flux and the self-consistent method for determining γ rebut the first two objections. Objection 3 is not very important if one uses a simple density correction on the moderator, as long as the slowing down density does not vary rapidly over the lattice. Objection 4 is important and our work will be directed at obtaining good kernel prescriptions.

In this section we will examine and compare values of γ with reference to their consistency with the arguments given above regarding the asymptotic flux and the self-consistent method.

Section 3.1 Calculations of γ in Graphite and D_2O

γ has been calculated by the self-consistent method for a cylindrical rod of 2 cm radius, of natural uranium in a graphite moderator. An infinite square lattice with minimum center-to-center distance "a" (the lattice pitch) has been considered. γ has been obtained as a function of a. Diffusion-age kernels have been used with the values of L^2 and τ previously given. f has been calculated by diffusion theory recipes, which are fairly accurate for low enrichment rod.

The results of γ as a function of a are presented in Table 2. It is clear that γ remains essentially constant as the lattice pitch is varied. These results indicate that γ is a rod property in a particular moderator and is independent of the spacing of the rods within the lattice, as the heterogeneous method postulates. Thus the self-consistent procedure using the asymptotic flux concept is consistent with the heterogeneous method.

A similar calculation has been made for a natural uranium rod of cylindrical cross section and radius 1.75 cm in a D_2O moderator. The D_2O kernel functions used were age-diffusion kernels with $L^2 = 13{,}456$, $\tau = 116$ cm^2
The thermal utilization was calculated, for each lattice pitch, by diffusion theory.

A table of values of γ for various lattice pitch values "a" is given in Table 3, as a is varied from 8 to 24 cm. Again one sees that γ remains essentially constant as the lattice pitch is varied. This confirms the heterogeneous assumption that γ is a property of the rod alone (in a particular moderator) and is independent of rod spacing. It also shows that the self-consistent method in D_2O is consistent with the heterogeneous method.

In order to make a direct comparison between γ's for the same rod in different moderators, a similar calculation was made for a cylindrical rod of 2 cm radius in D_2O. We obtained the result that $\gamma = .375\ cm^{-1}$, as compared with $\gamma = .267\ cm^{-1}$ in graphite.

Table 2

Variation of γ with Lattice Pitch in Graphite

Lattice Pitch	Thermal Utilization	
a in cm	f	$\gamma(a)$ cm^{-1}
10	.994	.251
15	.971	.264
20	.939	.266
25	.900	.269
30	.858	.270
40	.755	.267
50	.650	.266

Table 3

Variation of γ with Lattice Pitch in D_2O

Lattice Pitch	Thermal Utilization	
a in cm	f	$\gamma(a)$ in cm^{-1}
8.186	.9982	.572
12.279	.9950	.576
16.372	.9909	.579
20.465	.9848	.580
24.557	.9770	.580

Section 3.2 Comparison with Simple Physical Model

We now consider the relative values of the γ's for the same rod in two different moderators. For the 2 cm radius rod we have obtained

$$\gamma = 0.375 \quad \text{in} \quad D_2O$$

$$\gamma = 0.267 \quad \text{in} \quad \text{graphite.}$$

For equal number of absorptions, the asymptotic flux in the two infinite lattices, one with a D_2O moderator, the other with a graphite moderator, compare as follows according to (3.1)

$$\frac{\phi(D_2O)}{\phi(\text{graphite})} = \frac{0.375}{0.267} = 1.405$$

Since we consider identical rods in the two lattices the surface flux must be the same in the two rods in order to have equal numbers of absorptions. If γ were defined as the ratio of surface flux to absorptions it would be a rod property independent of the lattice. Since, however, we define it as the ratio of asymptotic flux (in the moderator) to absorptions it will depend on the moderator material as well as on the rod.

The asymptotic flux in the D_2O lattice must be higher than in the graphite lattice because the D_2O thermal absorption cross section is lower than that of graphite. In order to achieve the thermal utilization values from which the γ values were obtained, the moderator absorptions must bear a certain ratio to each other. This will fix the ratio of the asymptotic fluxes. Let the index 1 denote the D_2O lattice and the index 2

denote the graphite lattice. The ratio of moderator absorptions is

$$\frac{1-f_1}{1-f_2} = \frac{\sigma_{a1} \; V_1 \; \bar{\phi}_1}{\sigma_{a2} \; V_2 \; \bar{\phi}_2} \tag{3.1}$$

where f is the thermal utilization, $\bar{\phi}$ is the average flux in the moderator, V_1 is the moderator volume per unit cell, and σ_a is the thermal absorption cross section. Let us take

$$\frac{\sigma_{a1}}{\sigma_{a2}} = \frac{3.3 \times 10^{-5}}{26 \times 10^{-5}} \; , \qquad \frac{V_1}{V_2} = 1 .$$

For a lattice pitch of 16 cm, $f_1 = .9938$, $f_2 = .966$. Then from (3.10) one finds

$$\frac{\bar{\phi}_1}{\bar{\phi}_2} = \frac{.0062}{.034} \times 7.87 = 1.44$$

One would expect that the ratio of $\frac{\bar{\phi}_1}{\bar{\phi}_2}$ would be the same as the ratio of the asymptotic fluxes. Hence one obtains

$$\frac{\phi(D_2O)}{\phi(\text{graphite})} = 1.44$$

in agreement with the value derived from the ratio of the γ's.

Section 3.3 Dependence of A on the Moderator

The resonance escape probability for a single lumped U^{238} absorption resonance has been calculated for a 1.5 cm natural uranium rod in both D_2O and graphite moderators. The calculations were performed using the parameters for the fast neutron group in conjunction with $I_{eff}\left(\frac{\text{Resonance Absorptions/cm sec}}{\text{Av Flux at Rod Surface}}\right)$ determined experimentally. I_{eff} is the Effective Resonance Integral which is usually obtained in terms of mass and surface contributions.[14] The resonance escape probabilities were calculated using a diffusion equation for resonance neutrons, where the resonance flux at the surface of the rod was obtained in terms of the experimentally determined I_{eff}. In this way we avoid having to use the resonance properties of the fuel directly except for taking the lethargy width (U_r) of the lumped resonance equal to 3. The individual resonance escape probabilities (p) were then used in the previously derived expression.

$$A^{lumped} = (1-p)\, a^2 \qquad (3.2)$$

where a is the lattice pitch,

to determine the resonance absorption parameters A.

For the rod under consideration we found A = 52.0 for the graphite moderator and A = 17.3 for D_2O. This vast difference between the values of A for the same rod in two different moderators results for the most part from our original definition of A which is the ratio of the resonance absorptions to the asymptotic

slowing down density rather than to the epithermal flux at the surface. We will now show that for the same slowing down density, the flux in graphite is approximately three times as large as in D_2O. Therefore, we would expect approximately three times as many absorptions for the rod in graphite than in D_2O since we expect the absorptions to be proportional to the flux at the rod surface. To determine the approximate flux ratio we use

$$q = \xi\sigma_s\phi \tag{3.3}$$

for each of the two moderators. Relating them, we have,

$$\frac{\phi_{D_2O}}{\phi_{graphite}} = \left[\frac{q_{D_2O}}{q_{graphite}}\right] \left[\frac{(\xi\sigma_s)_{graphite}}{(\xi\sigma_s)_{D_2O}}\right] \tag{3.4}$$

Assuming the slowing down densities are the same in the two moderators, we evaluate the second parenthesis on the right to obtain $\frac{\phi_{graphite}}{\phi_{D_2O}} = 2.66$.

It should be noted that in the above development we assumed the ratio of the asymptotic slowing down densities in the two moderators was the same as the actual slowing down densities. Thus the resonance flux depression due to the rod was not taken into account. This resonance flux depression is more important in graphite (where resonance absorption is higher than in D_2O). This probably explains the discrepancy between the factors of 2.66 and 3. To calculate the approximate ratio of the A's for

the same rod in two moderators we use the following expression

$$\frac{A_{mod_1}}{A_{mod_2}} \approx \frac{\left[\frac{\text{rod absorptions}}{\phi\ (\text{surface})}\right]_{mod_1} \cdot \left[\frac{\phi\ \text{surface}}{q\ \text{asymptotic}}\right]_{mod_1}}{\left[\frac{\text{rod absorptions}}{\phi\ (\text{surface})}\right]_{mod_2} \cdot \left[\frac{\phi\ \text{surface}}{q\ \text{asymptotic}}\right]_{mod_2}} \qquad (3.5)$$

The first term in both the numerator and denominator depends only on the rod and not on the moderator. Thus using equation 3.3 we have

$$\frac{A_{mod_1}}{A_{mod_2}} \approx \frac{(\xi\sigma_s)_{mod_2} \left[\frac{\phi_{(surface)}}{\phi_{(asymptotic)}}\right]_1}{(\xi\sigma_s)_{mod_1} \left[\frac{\phi_{(surface)}}{\phi_{(asymptotic)}}\right]_2} \qquad (3.6)$$

Letting the index 1 denote D_2O and 2 denote graphite one has

$$\frac{A_1}{A_2} = 2.66 \frac{\left[\frac{\phi_{(surface)}}{\phi_{(asymptotic)}}\right]_{D_2O}}{\left[\frac{\phi_{(surface)}}{\phi_{(asymptotic)}}\right]_{graphite}}$$

Because the $\frac{\phi_{(surface)}}{\phi_{(asymptotic)}}$ is greater in D_2O than in graphite we see that the ratio of the A's must be greater than 2.66, therefore the value of 3 given by use of equation (3.2) is reasonable.

The greater flux depression in graphite results from the higher resonance absorption rate at the higher energy resonances, due to the larger flux per unit slowing down density. Thus if A's were calculated for each individual resonance instead of lumping the resonances together, this correction factor would not be needed.

Section 4 Heterogeneous Calculations in D_2O Systems

In this section are presented results for some problems in which the heterogeneous nature of the core is particularly important. Similar results have previously been presented for graphite moderated systems.

Section 4.1 Calculations of Infinite Complex Lattices in D_2O

HERESY 1 calculations have been performed on complex lattices in D_2O consisting of two superimposed infinite square lattices. Results for the same type of calculations were presented in Quarterly No. 2 for graphite. However, in the present computations, the pitch of the more close packed of the two superimposed lattices was taken as 16cm as compared with 20 cm in the graphite problem. Figure 1 of Quarterly No. 2 shows the configurations I and II, which have a pitch ratio between the two superimposed square lattices of 1/1 and 2/1 respectively. In Table 4 we cite the results for the two configurations in D_2O when the rods of both superimposed lattices are unenriched or enriched and in the last 2 columns (complex lattice) we consider what happens when the enriched rods and unenriched rods are intermeshed. In case II of the complex lattice study, we took the pitch of the enriched rods to be twice that of the unenriched rods and not vice-versa.

Comparing the reactivities when all the rods are of one type, we find that the tight packed configuration has a lower k than the loose packed configuration. By continuing an analysis of this type further we could determine an optimum packing for an infinite lattice. For the case of the tight packed complex lattice we do obtain a small increase in k over the more loosely packed configuration. However, this small gain is only obtained

with a large loss in Average Power/Max. Power because the unenriched rods feel the sink effect of the four enriched rods in their immediate vicinity in the tight packed case.

Table 4

Calculation Results for a Complex Lattice in D_2O

	Unenriched Lattice		Enriched Lattice		Complex Lattice	
Geometry	I	II	I	II	I	II
k	1.147	1.206	1.3762	1.451	1.283	1.265
$\frac{\text{Average Power}}{\text{Maximum Power}}$	1.	.9754	1	.8549	.8106	.9533
i_2/i_1	1.	.8769	1	.8186	1.610	1.304
$\overline{\eta}$	1.34	1.34	1.605	1.605	1.503	1.562
p	.8593	.9116	.8593	.8990	.8593	.9304
f	.9961	.9874	.9978	1.006	.9932	.8703

Section 4.2 Approach to Criticality of a Square Lattice in D_2O

Calculations of reactivity and power distributions in progressively larger square lattices of natural uranium rods have been extended to the case where the moderator and infinite reflector are composed of D_2O. (In Quarterly III, this study was performed for a graphite moderator). The rod parameters and D_2O diffusion-age kernel input parameters are given below:

$$\eta = 1.34$$
$$\gamma = .580 \text{ cm}^{-1}$$
$$A = 18 \text{ cm}^2$$
$$R_o = 1.75 \text{ cm}$$

$$L = 116 \text{ cm}$$
$$\Sigma_a = 3.97 \times 10^{-5} \text{ cm}^{-1}$$
$$\tau = 116 \text{ cm}^2$$
$$\tau_r = 87 \text{ cm}^2$$

The lattice pitch in all configurations was taken as 16 cm. The configurations studied were progressively larger square arrays containing 8, 9, 25, 49 and 81 rods. These are the same configurations 1A, 1B, 2B, 4 and 5 referred to in the last quarterly except that the lattice pitch is now 16 cm. These configurations are reproduced in figures 1-4 of this report. The objects of this study are two-fold:

a) To show how the heterogeneous method can be used to estimate the critical mass or to determine the number of rods necessary to obtain any desired reactivity once the rod type and vol. U/vol. D_2O have been selected. Calculations similar to those cited could be used to determine the vol. U/vol. D_2O ratio (lattice pitch) which would maximize k for a particular rod under study. In this manner one could make a complete design study for a particular rod-moderator combination.

b) To study the individual peculiarities of the power distribution.

The qualitative results for D_2O moderator are very similar to those obtained for graphite. In both cases k increases rapidly as the number of rods is increased. After we have about 25 rods in the lattice, the rate of increase of k with N(number of Rods) becomes much slower.(Fig. 5). It should be noted that to directly compare critical masses for the D_2O and graphite moderators, each rod in D_2O is equivalent to 1.306 rods in graphite since the natural uranium rods were taken as having larger radii in the D_2O moderator -- 2 cm, as compared with 1.75 cm in graphite.

We cite the HERESY 1 D_2O results below.

Configuration 1A: 3 by 3 array with a lattice spacing of 16 cm. Central rod absent. The geometry is shown in Fig. 1. The numbers

of the various rods distinguish different rod symmetries. All rods with the same number have the same spatial symmetry. This notation will be used throughout the report.

Results for Configuration 1A

$k = .9437$

$p = .9617$

$f = .7323$

$\bar{i} = .9833$

$i_1 = 1.000$

$i_2 = .9665$

Configuration 1B: 3 by 3 array with a lattice spacing of 16 cm. Central rod present. The geometry is shown in Fig. 1.

Results for Configuration 1B

$k = .9580$

$p = .9539$

$f = .7495$

$i = .9833$

$i_1 = .9971$

$i_2 = 1.000$

$i_3 = .9846$

Configuration 2B: 5 by 5 array with central rod present. The pitch is 16 cm. The geometry is shown in Fig. 2.

Results for Configuration 2B

$k = 1.093$

$p = .9445$

$f = .8636$

$\bar{i} = .9268$

$i_1 = .9650$

$i_2 = .9318$

$i_3 = .9404$

$i_4 = .8838$

$i_5 = .9106$

$i_6 = 1.000$

Configuration 4: 7 by 7 array. The geometry is shown in Fig. 3.

Results for Configuration 4

$k = 1.147$

$p = .9401$

$f = .9104$

$\bar{i} = .8776$

$i_1 = .9774$

$i_2 = .9554$

$i_3 = .9133$

$i_4 = .8368$

$i_5 = .8934$

$i_6 = 1.000$

$i_7 = .7858$

$i_8 = .8144$

$i_9 = .8660$

$i_{10} = .8841$

Configuration 5: 9 by 9 array. The geometry is shown in Fig. 4.

Results for Configuration 5

$k = 1.195$

$p = .9584$

$f = .9308$

$\bar{I} = .7959$

$i_1 = .9790$

$i_2 = .9634$

$i_3 = .9248$

$i_4 = .8626$

$i_5 = .9126$

$i_6 = 1.0000$

$i_7 = .7133$

$i_8 = .7840$

$i_9 = .8278$

$i_{10} = .8441$

$i_{11} = .5843$

$i_{12} = .6449$

$i_{13} = .7055$

$i_{14} = .7430$

$i_{15} = .7564$

The relative absorption results for configurations 1A and 1B indicate that the insertion of the central rod depresses the flux sufficiently at its nearest neighbors to give the corner

rods the highest power density. This is the same result observed in graphite. As we go to larger arrays we find the k increases, f increases, p decreases and the central rod always has the greatest number of neutron absorptions. These are qualitatively the same results encountered when we considered a graphite moderator.

Fig. 1 Rod Symmetries in Configuration 1A and 1B

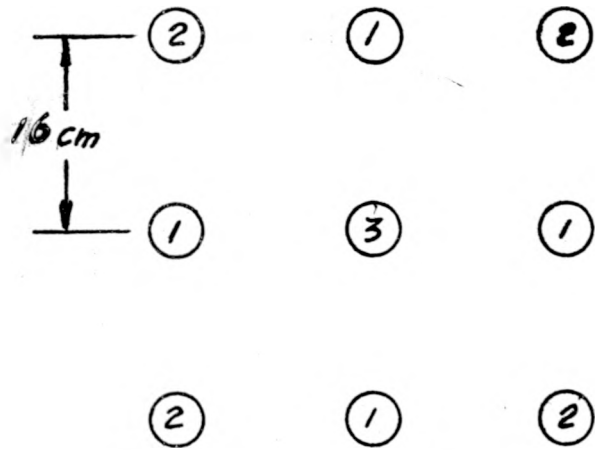

Fig. 2 Rod Symmetries in Configuration 2B

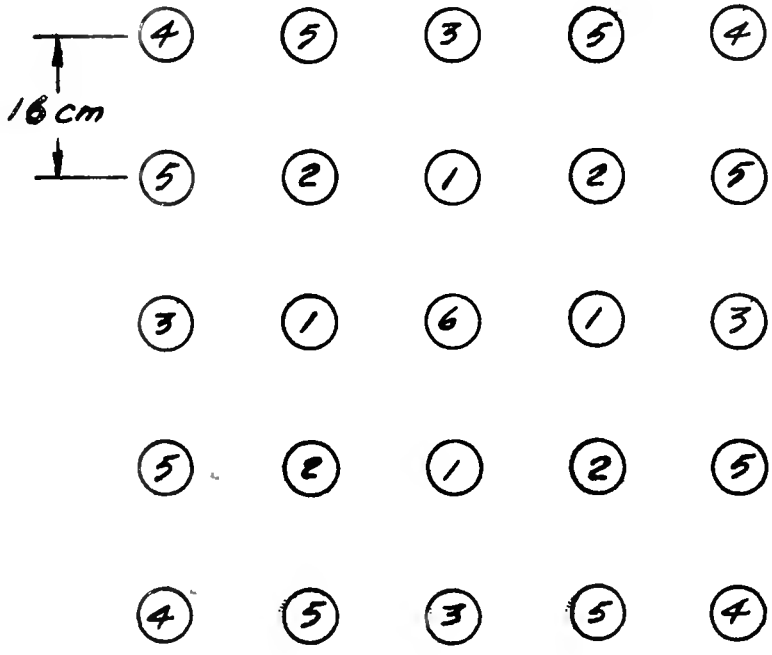

Fig. 3 Rod Symmetries in Configuration 4

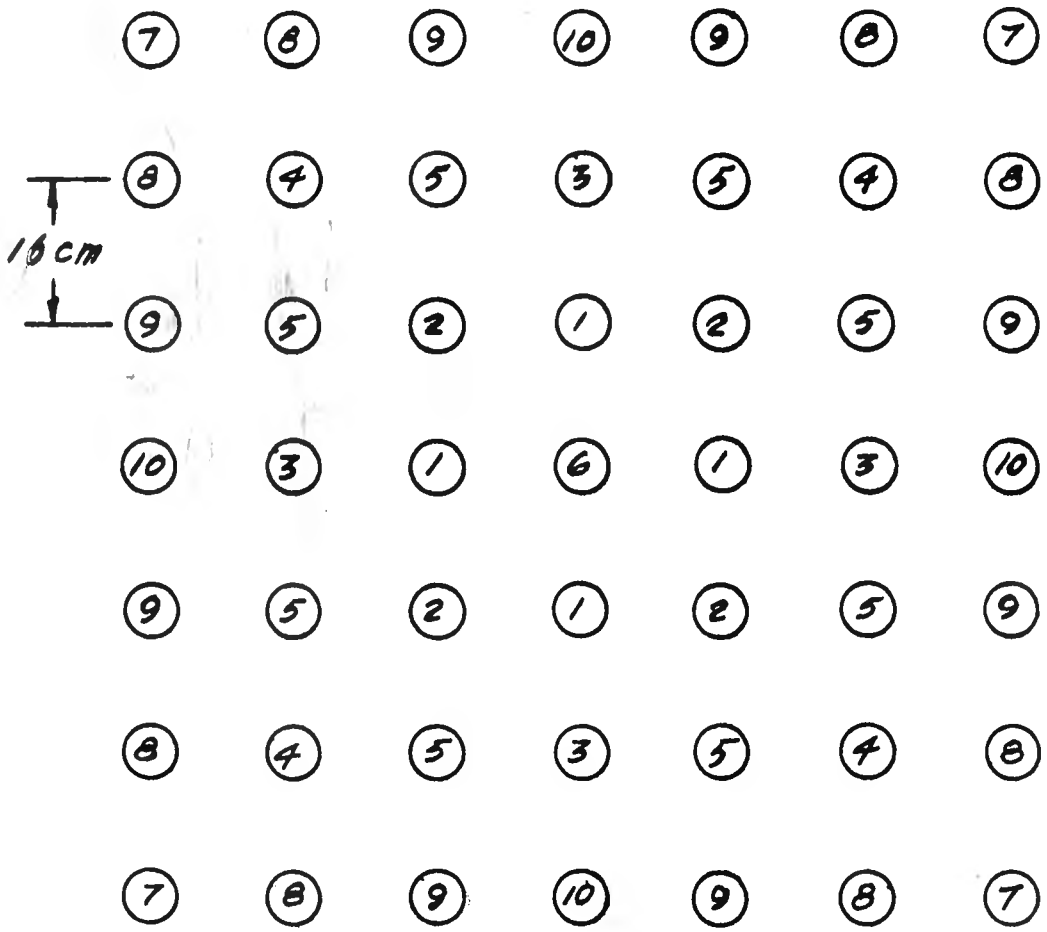

Fig. 4 Rod Symmetries in Configuration 5

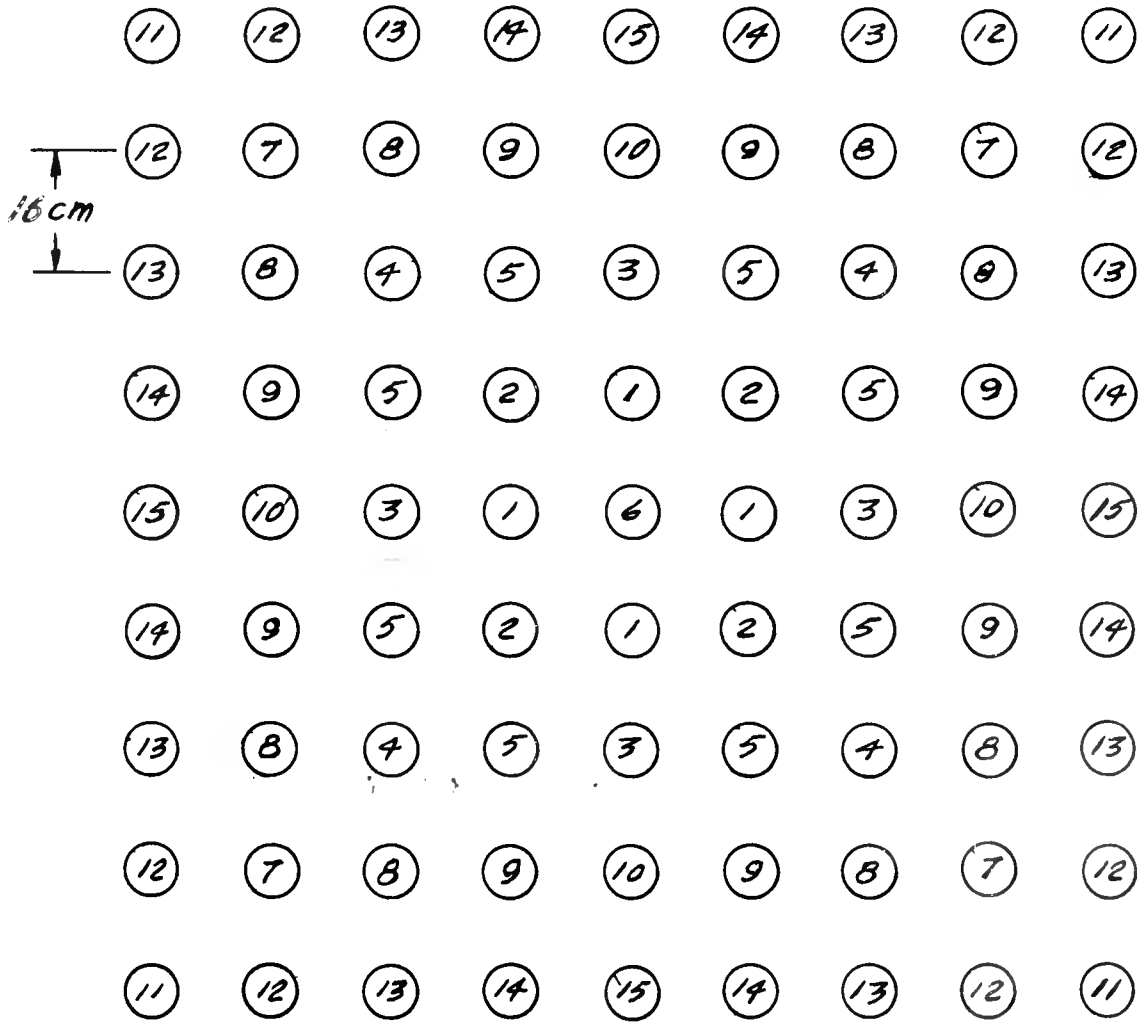

Fig. 5 Reactivity vs Number of Rods Present in Square Arrays in Graphite and D_2O.

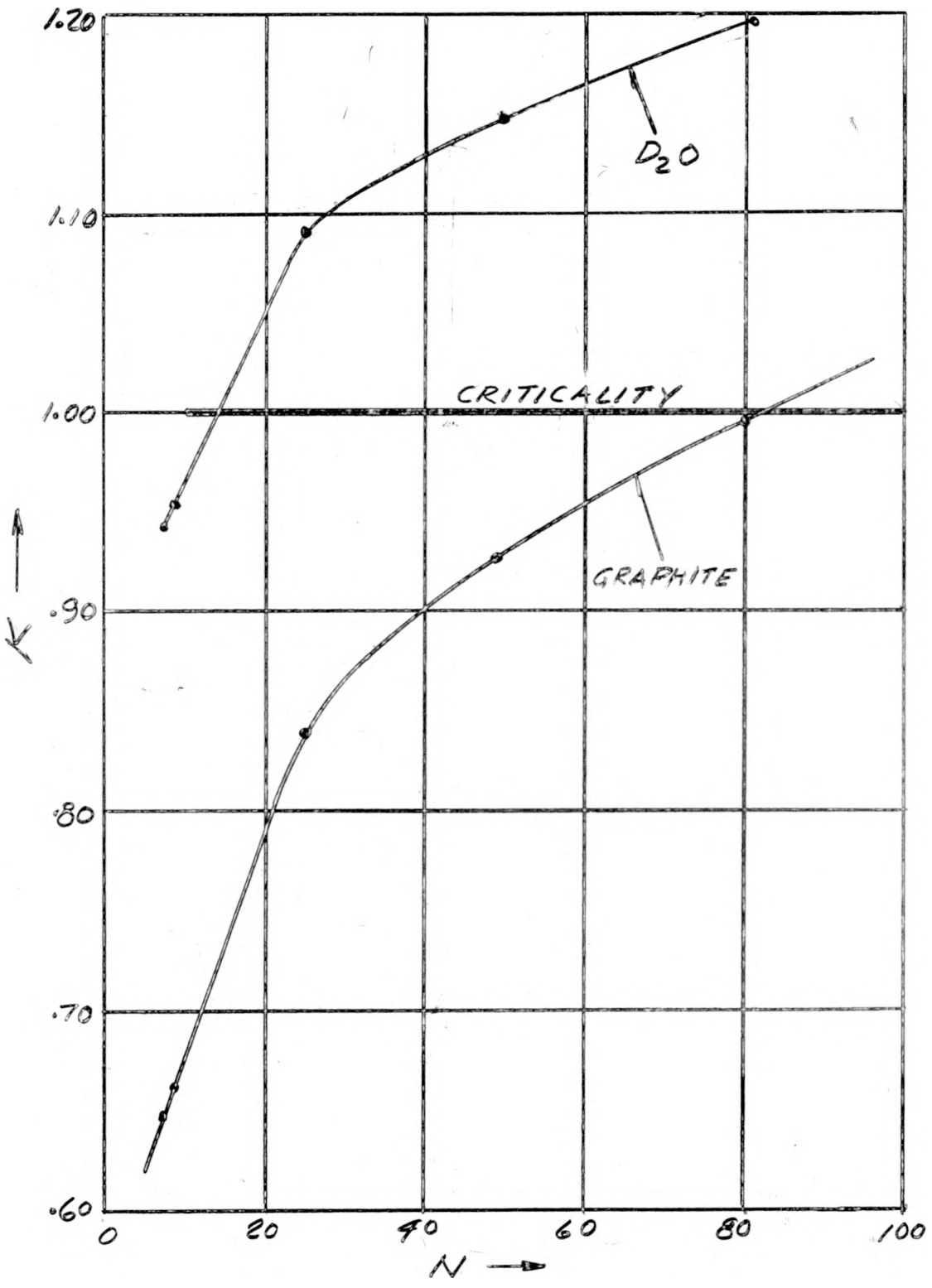

Section 4.3 Study of Spiked D_2O Cores

A spiked core study similar to that made with a graphite moderator has been performed for the 49 rod square lattice configuration in D_2O. (Configuration 4 with a lattice pitch = 16 cm.) In each of the problems, 12 of the natural uranium rods were replaced by 1.3% enriched uranium rods. By distributing the enriched rods in various ways, the reactivity and the average to maximum power ratio can be varied considerably (Fig. 6).

The qualitative results of spiking were common to both D_2O and graphite lattices and indicated that enriching rods located near the outside of the core leads to a flatter pattern and lower reactivity than if the rods on the inside are enriched. When rods on the outside are enriched, the resonance escape probability is higher since the additional fast neutrons emitted from these rods see less of the core during slowing down than if they were emitted from an inner rod. However, these additional neutrons which slow down in the reflector are much more likely to be absorbed in the reflector when they become thermal. Thus enriching rods on the outside of the core, leads to a lower thermal utilization. This lower thermal utilization greatly outweighs the increased resonance escape probability when the enriched rods are on the outside. Therefore, we have a lower reactivity for this case. Since in the unspiked core the rods with the lowest absorptions are located away from the reactor center it is to be expected that

enriching these rods will lead to a flatter flux than if the inner rods are enriched. For a discussion of how the core designer would apply the heterogeneous method iteratively to determine flatter power distribution, you are referred to Quarterly No. 3.

The configurations studied are shown in figures 7 to 11. The natural uranium rods and the D_2O moderator have the same properties as described in the last section. The enriched rod parameters are as follows:

$$\eta = 1.605$$

$$\gamma = .232$$

$$A = 18$$

$$R_o = 1.75 \text{ cm}$$

The calculation results for these 5 configurations are given in Table 5.

Table 5

D_2O Spiked Core Results

Enriched Rod Symmetries	8,10	4,9
Configuration No.	17	18
k	1.222	1.224
η	1.424	1.424
p	.9416	.9407
f	.9117	.9141
Average Power/Max. Power	.7464	.7615
i_1 (4 rods)	.7083	.7388
i_2 (4 rods)	.7030	.7300
i_3 (4 rods)	.6797	.7123
i_4 (4 rods)	.6398	.9482
i_5 (8 rods)	.6801	.6844
i_6 (1 rod)	.7133	.7440
i_7 (4 rods)	.6375	.6483
i_8 (8 rods)	.9428	.6482
i_9 (8 rods)	.6756	1.000
i_{10} (4 rods)	1.000	.6993

Table 5 (continued)

Enriched Rod Symmetries	1,2,3	1,4,10	2,3,7
Configuration No.	19	20	21
k	1.244	1.232	1.229
η	1.435	1.427	1.425
p	.9381	.9395	.9400
f	.9242	.9188	.9172
Average Power/Max.Power	.6545	.6733	.6968
i_1	1.000	1.000	.6983
i_2	.9666	.6655	1.000
i_3	.8969	.6317	.9430
i_4	.5544	.8271	.6036
i_5	.6012	.6209	.6320
i_6	.7267	.6872	.7462
i_7	.4819	.5347	.8081
i_8	.5141	.5528	.5792
i_9	.5639	.5946	.6232
i_{10}	.5757	.8804	.6277

Fig. 6 Average to Maximum Power vs K-1 for Spiked D_2O Lattices

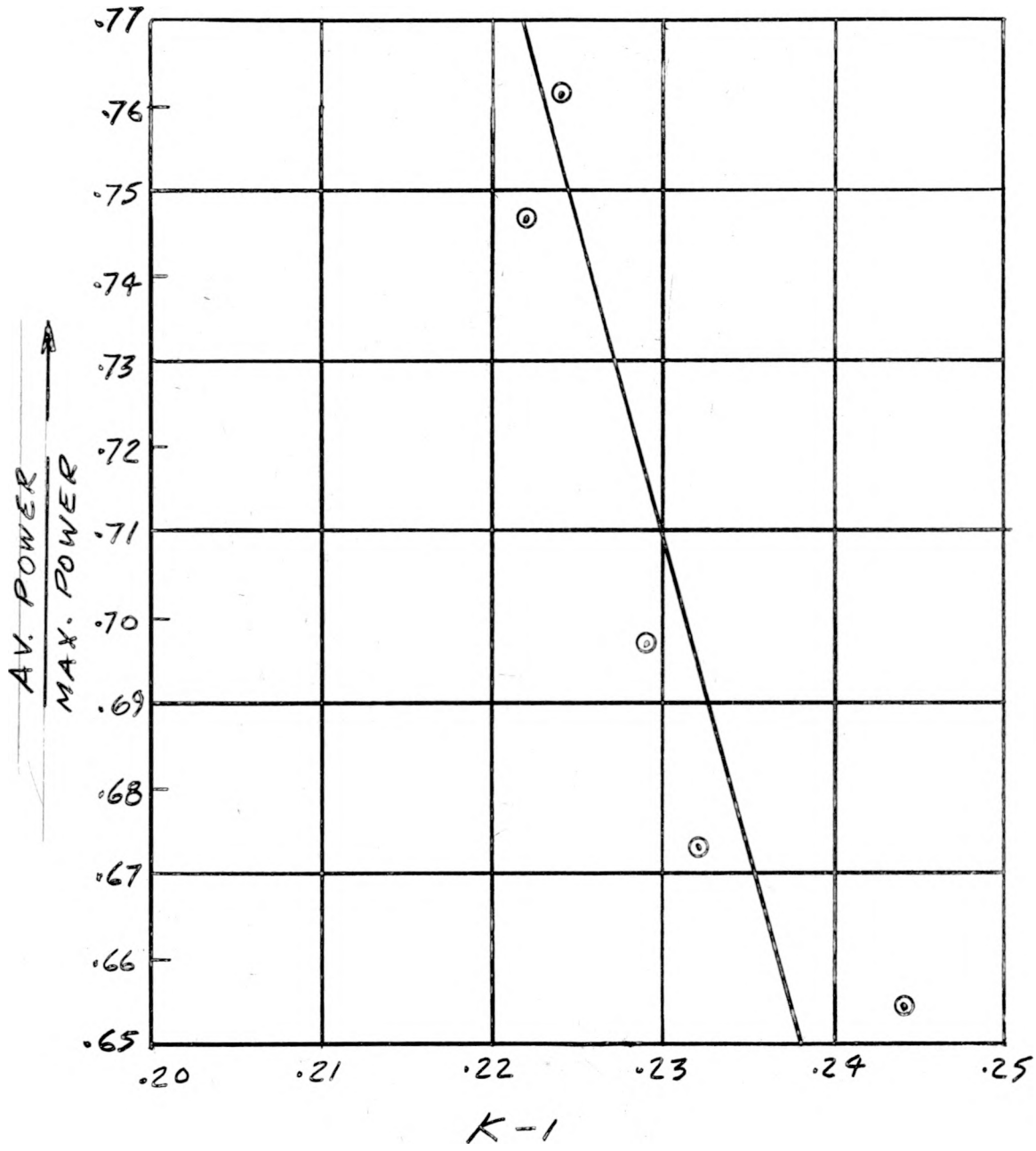

The next 5 figures represent the lower right hand quadrant of Configuration 4 (Quarterly No. 3) where 12 of the natural uranium rods have been replaced by rods of 1.3% enriched uranium. The enriched rods are indicated by a heavy ring.

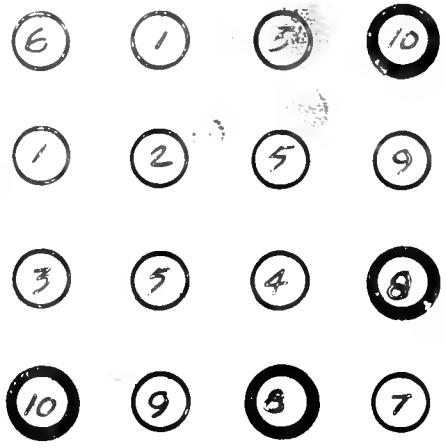

Fig. 7 Configuration 17

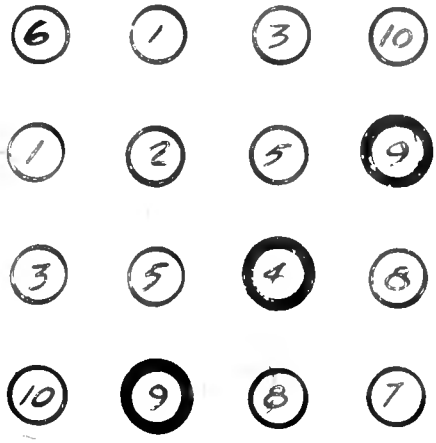

Fig. 8 Configuration 18

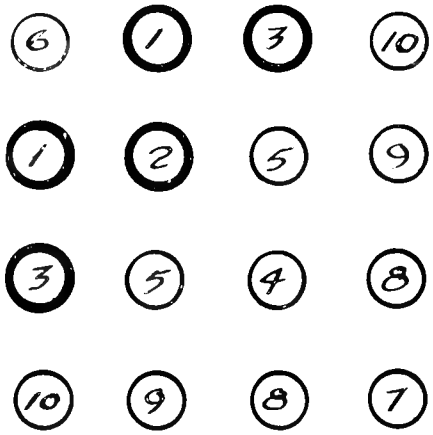

Fig. 9 Configuration 19

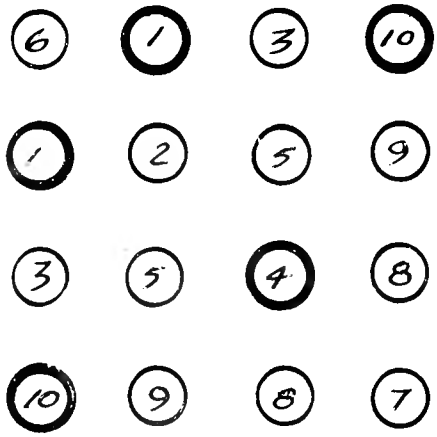

Fig. 10 Configuration 20

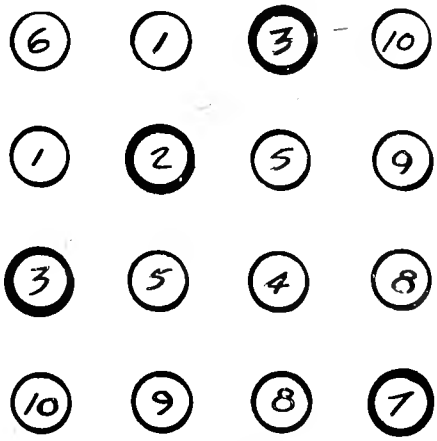

Fig. 11 Configuration 21

Section 5 Comparison of Hexagonal and Square Lattices

We have previously calculated the approach to criticality of a square lattice of natural uranium rods (radius 2 cm) in an infinite graphite moderator. Calculations have now been performed on hexagonal arrays of the same rod in a graphite moderator; the configurations representing progressively larger cores. In order to make a direct comparison between square and hexagonal arrays, we have chosen the (vol. U/vol. mod) in the equivalent cell to be the same for both cases. The equivalent hexagonal lattice obeying this condition has

$$a_H = .877\ a_S$$

where a_S is the pitch of the square lattice, and a_H is the lattice dimension of the hexagonal array. This gives $a_H = 17.54$ cm as compared with $a_S = 20$ cm.

Calculations have been performed on hexagonal arrays with 10, 25, 46 and 82 rods. In Fig. 12, we show the positions of the rods, specified according to rod type in our hexagonal generating routine.

Our rods are numbered in such a fashion that any rod of type j is further from the center rod than any rod of type i if $j > i$. In a few cases rods of type i and i + 1 are the same distance from the center rod. All the computations included the center rod (as in the square arrays) and the 4 hexagonal configurations studied can be readily obtained from Figure 12

by including only those rods belonging to types 1 and 2 (10 rod problem); 1 through 6 (25 rod problem); 1 through 10 (46 rod problem); and 1 through 17 (82 rod problem).

The results obtained for the hexagonal array as compared to the square array (Table 6) show very little, if any, advantage of one configuration over the other. In the cases where the number of rods are practically the same (25 and 81 or 82 rods) the results indicate that the reactivity of the square configuration may be a fraction of a per cent higher than for the hexagonal array. This seems to be due to a slightly higher thermal utilization for the square lattice symmetry. From Figure 13 we see that the reactivity buildup for both square and hexagonal arrays can be accurately plotted on one curve. The same result can be seen to hold for $\bar{i}$.

In Table 7, we tabulate the results for the absorption pattern for the hexagonal lattices studied. It is immediately evident that when a rod is on the outside of the core, it has a much higher relative absorption rate than if more rods are included on the exterior of the one under consideration. For instance, a rod of type 6 in the 25 rod configuration has approximately a 10% higher relative absorption rate than when the rod is a part of the 46 rod configuration. This is because those neutrons scattered back from the reflector have a high probability for capture in the exterior rods. In the 10 rod configuration, the outside rods (type 2) have the highest

absorption rate.

Let us now compare the absorptions in the 25 rod square and hexagonal lattices. Both lattices are shown in Figure 14. The relative absorptions in the square lattice have formerly been found to be:

$$i_c = 1.000$$
$$i_1 = .954$$
$$i_2 = .910$$
$$i_3 = .934$$
$$i_4 = .856$$
$$i_5 = .893$$

Since rods of type 1 in both hexagonal and square arrays are approximately the same distance from the center rod and have all the other rods exterior to them, we might expect the absorption to be about the same in the two cases. From a comparison of our results we see that this is true. Rods of type 2 in both configurations also have approximately the same absorptions. Rods of type 6 in the hexagonal configuration have such a high relative absorption rate because they see not only those neutrons scattered back from the reflector, but also have a high probability of capturing those neutrons scattered in their direction from within the core since the only shielding (sink) effect comes from rods of type 3.

Table 6

Comparison of HERESY 1 Results for Square and Hexagonal Lattices as we Approach Criticality

No. of Rods	Hexagonal or Square	Av.Power / Max.Power	k	p	f
9	Square	.9820	.6630	.9300	.5290
10	Hex.	.9707	.6866	.9353	.5479
25	Square	.910	.8428	.9117	.6899
25	Hex.	.9152	.8416	.9121	.6866
46	Hex.	.8367	.9211	.9014	.7626
49	Square	.8200	.9272	.8998	.7696
81	Square	.7670	.9772	.8927	.8167
82	Hex.	.7680	.9757	.8921	.8162

Table 7

Absorption Patterns for Hexagonal Lattices

Absorptions	10 rods	25 rods	46 rods	82 rods
i_c	.9299	1.000	1.000	1.000
i_1	.9257	.9614	.9725	.9825
i_2	1.000	.9141	.9186	.9473
i_3		.9048	.8925	.9291
i_4		.9002	.8304	.8791
i_5		.8590	.8063	.8468
i_6		.9394	.8110	.8418
i_7			.7617	.7954
i_8			.8111	.7768
i_9			.8169	.7382
i_{10}			.7769	.7116
i_{11}				.6891
i_{12}				.6862
i_{13}				.7079
i_{14}				.6927
i_{15}				.6815
i_{16}				.6466
i_{17}				.5998

Fig. 13 Plot of K and Av. Power/Max. Power vs N(Number of Rods)

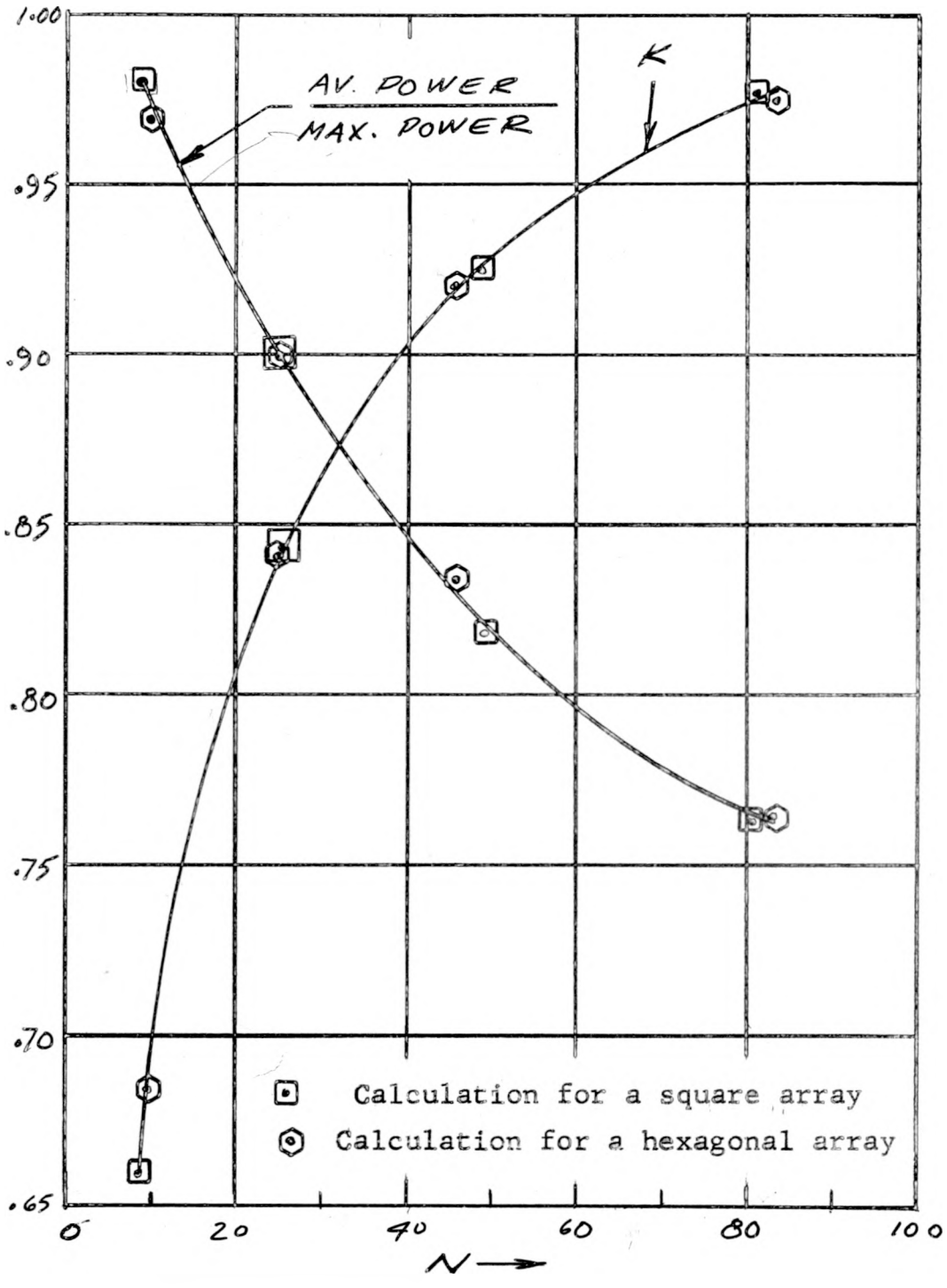

Fig. 14 Hexagonal and Square Arrays of 25 Rods

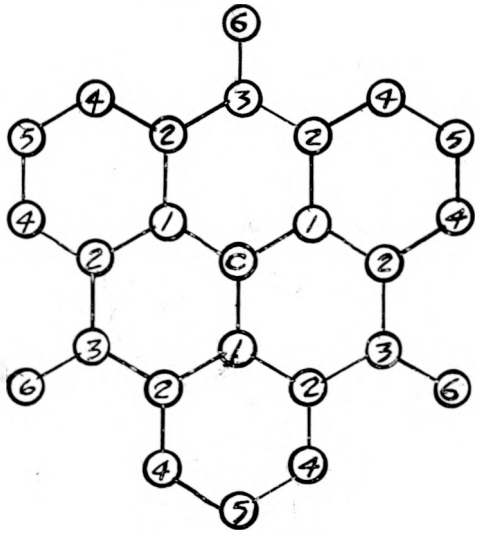

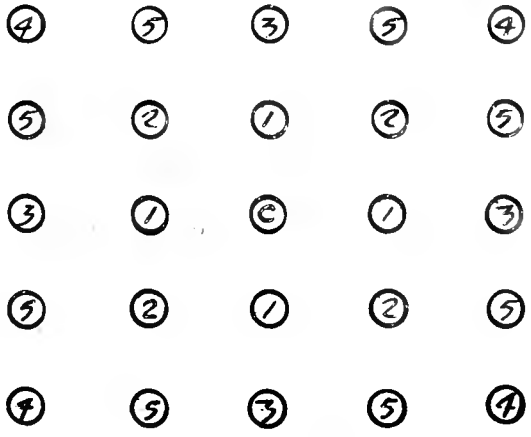

Appendix I: Notation

In this appendix we shall define the matrices used in the equations of HERESY 1.

$\underline{\gamma}$ is a diagonal matrix whose diagonal elements are the values γ_n (thermal neutron absorption parameters) for each of the rod types.

The $\underline{Z}$ matrix is obtained from the thermal diffusion kernel f_{nm}. We shall designate rod types by a Roman letter subscript and a particular rod of that type by a Greek letter subscript. Thus f_{nm} will be written with four indices, $f_{n\alpha,m\beta}$, the two to the right of the comma referring to the source rod (the β rod of the m-th type), the two to the left of the comma referring to the receiver rod (the α rod of the n-th type). Then the element Z_{nm} of the matrix is defined as

$$Z_{nm} = \sum_{\beta} f_{n\alpha,m\beta} \qquad (2.2)$$

the summation extending over all rods of the m-th type. Note that Z_{nm} is independent of α because of symmetry.

The $\underline{G}$ matrix represents slowing down from fission followed by thermal diffusion, with corrections for the flux diminution due to resonance absorption. Designating the convolution of the slowing down kernel for fission neutrons with the diffusion kernel as F_{ab} and the same convolution when the neutrons are considered born at the energy of the equivalent lumped resonance

as F^r_{ab} we define the matrices

$\underline{\underline{T}}$, with components $T_{nm} = \sum_{\beta} F_{n\alpha,m\beta}$

$\underline{\underline{T}}^r$, with components $T^r_{nm} = \sum_{\beta} F^r_{n\alpha,m\beta}$.

The slowing down kernel to the equivalent resonance is designated by $g^{(r-1)}_{ab}$. We define

$\underline{\underline{S}}^r$, with components $S^r_{nm} = \sum_{\beta} g^{(r-1)}_{n\alpha,m\beta}$.

We also have the resonance absorption parameter matrix,

$\underline{\underline{A}}^r$, a diagonal matrix with components A_m.

Appendix II. Calculation of Slowing Down Kernels and Matrices

In this appendix we shall derive recursion relations to calculate the matrices $\underline{\underline{S}}^r$ giving the slowing down densities at the r-th resonance energy at the various rod types. Thus S^r_{nm} is the slowing down density at the r-th resonance energy at the rod type n due to a fission at rod type m. The $\underline{\underline{S}}^r$ matrices are needed in HERESY 2 calculations. We shall also derive recursion relations to calculate the matrices $\underline{\underline{T}}^r$ whose element T^r_{nm} give the depletion of the thermal flux at rod type n due to absorption of a neutron at resonance energy r at rod type m.

We shall assume that a slowing down density function $g_{ab}(P\rightarrow q)$ for an infinite moderator is known and tabulated. $g_{ab}(P\rightarrow q)$ is the slowing down density for one neutron per sec starting out from rod b with energy P (an order number for the energy levels of interest) at rod a and at energy q. Similarly, we shall assume that a function $F_{ab}(P\rightarrow\text{thermal})$ for an infinite moderator is known and tabulated. $F_{ab}(P\rightarrow\text{thermal})$ gives the thermal flux at rod a due to one neutron per sec starting out from rod b at energy P. Both $g_{ab}(P\rightarrow q)$ and $F_{ab}(P\rightarrow\text{thermal})$ depend on the distance from rod a to rod b. For a particular rod configuration one can set up rod to rod matrices $\underline{\underline{g}}(P\rightarrow q)$ and $\underline{\underline{F}}(P\rightarrow\text{thermal})$ of these functions.

We shall also define a rod-to-rod matrix $\underline{\underline{g}}^P(o\rightarrow P+1)$. This is the matrix of slowing down densities which have escaped the

first P resonances in slowing down from the source energy (denoted by zero) to the energy just above the P+1 resonance. The elements of this matrix $g^{P}_{nm}(o \to P+1)$ give the asymptotic slowing down density near the n-th rod if the source is located at the m-th rod. Similarly, one can define a rod-to-rod matrix $\underline{\underline{g}}^{P}(o \to r)$ where r is any resonance beyond the P + 1. This matrix gives the slowing down density through the first P resonances at the energy just above the r-th resonance if it is imagined that the resonances from P + 1 to r are non-existent.

One can now write a simple recursion relation between the $\underline{\underline{g}}$ matrices equivalent to equation (2.1) of the first quarterly report in this program.

$$\underline{\underline{g}}^{P}(o \to P+1) = \underline{\underline{g}}^{P-1}(o \to P+1) - \underline{\underline{g}}(P \to P+1) \cdot \underline{\underline{A}}^{P} \cdot \underline{\underline{g}}^{P-1}(o \to P) \qquad \text{(II.1)}$$

The matrix $\underline{\underline{A}}^{P}$ is taken to be a rod-to-rod matrix in this equation. Let us consider the successive matrices $\underline{\underline{g}}^{P}(o \to r)$ for all $r > P$. Equation (II.1) gives a recursion relation that permits us to calculate $\underline{\underline{g}}^{P}(o \to r)$ once we have $\underline{\underline{g}}^{P-1}(o \to r)$.

Equation (II.1) may be rewritten in a simpler form.

$$\underline{\underline{g}}^{P}(o \to P+1) = \underline{\underline{g}}(o \to P+1) - \sum_{n=1}^{P} g(n \to P+1)\underline{\underline{A}}^{n}\ \underline{\underline{g}}^{n-1}(o \to n) \qquad \text{(II.2)}$$

The summation is over the first P resonances.

We wish to calculate the matrix $\underline{\underline{S}}^{P}$ which is a type-to-type matrix. $\underline{\underline{S}}^{P}$ is defined as follows:

$$S^{P}_{nm} = \sum_{\beta} g^{P-1}_{n\alpha,m\beta}(o\rightarrow P) \qquad (II.3)$$

where the summation over β includes all rods of the m-th type. Summing over all rods of the same type in (II.2)

$$\underline{\underline{S}}^{P+1} = \underline{\underline{S}}'(o\rightarrow P+1) - \sum_{t=1}^{P} \underline{\underline{S}}'(t\rightarrow P+1) \cdot \underline{\underline{A}}^{t} \cdot \underline{\underline{S}}^{t} \qquad (II.4)$$

$\underline{\underline{A}}^{t}$ in this equation is the type-to-type resonance absorption matrix used in the body of this report. The $\underline{\underline{S}}'$ matrix is defined as follows:

$$S'_{nm}(P\rightarrow q) = \sum_{\beta} g_{n\alpha,m\beta}(P\rightarrow q) \qquad (II.5)$$

where the summation over β includes all rods of the m-th type.

Equation (II.4) rigorously requires the calculation of $\frac{1}{2} \cdot R \cdot (R-1)$ matrices $\underline{\underline{S}}'$, where R is the total number of resonances. In most cases, however, one will be able to use physical intuition to reduce the number of matrices required by a large factor. For example, if all the resonances are closely spaced in lethargy the slowing down lengths from one resonance to another will be small compared to the inter-rod spacing. Hence only the diagonal elements of S'(t→P+1) will be appreciable and these will each be equal to the number of rods in each type.

We now consider the recursion formula for the $\underline{\underline{T}}^{r}$ matrices. We first calculate the rod-to-rod matrix $\underline{\underline{F}}^{R-r}(r\rightarrow R+1)$ analogous to the $\underline{g}^{r}(o\rightarrow r+1)$ matrix, where R+1 denotes thermal energy. We note that the function F(P→R+1) is the convolution of g(P→R+1)

with the thermal diffusion kernel, and that therefore $F^{R-r}(r\to R+1)$ is the convolution of $g^{R-r}(r\to R+1)$ with the thermal diffusion kernel. An equation analogous (II.2) can be written for the matrices $\underline{\underline{F}}^{R-r}(r\to R+1)$.

$$\underline{\underline{F}}^{R-r}(r\to R+1) = F(r\to R+1) - \sum_{t=r+1}^{R} \underline{\underline{F}}(t\to R+1)\underline{\underline{A}}^{t}\underline{\underline{g}}^{t-r-1}(r\to t) \qquad (II.6)$$

We define the $\underline{\underline{T}}^{r}$ type-to-type matrix by

$$T^{r}_{nm} = \sum_{\beta} F^{R-r}_{n\alpha,m\beta}(r\to R+1) \qquad (II.7)$$

Summing over all rods of one type equation(II.6) takes the following form

$$\underline{\underline{T}}^{r} = T'(r\to R+1) - \sum_{t=r+1}^{R} \underline{\underline{T}}'(t\to R+1)\underline{\underline{A}}^{t}\ \underline{\underline{S}}^{t-r}(r\to t) \qquad (II.8)$$

Equation (II.8) can be used to calculate the $\underline{\underline{T}}^{r}$ matrices from the $\underline{\underline{S}}$ matrices calculated via (II.4) (with origin taken at the r-th resonance energy) and from the $\underline{\underline{T}}'$ matrix. The $\underline{\underline{T}}'$matrix is defined as follows in terms of the F function

$$T'_{nm}(P\to R+1) = \sum_{\beta} F_{n\alpha,m\beta}(P\to \text{thermal}) \qquad (II.9)$$

Thus equations (II.4) and (II.8) provide recursion relations for calculating the $\underline{\underline{S}}^{r}$ and $\underline{\underline{T}}^{r}$type-to-type matrices. It is only necessary to specify

1) the fundamental slowing down kernel $g_{ab}(P\to q)$ in tabular form

2) the fundamental slowing down-thermal diffusion convolution kernel F_{ab}(P→thermal)

3) the $\underline{\underline{A}}^r$ matrices

4) the geometric configuration of the rods

References

1. Klahr, C. N., Mendelsohn, L. B., Heitner, J., "Heterogeneous Reactor Calculation Methods" Quarterly Report No. 3, NYO-2675, December 31, 1959

2. Calculations for a graphite moderator are given in Reference 1 and in the following reference:
Klahr, C. N., and Mendelsohn, L. B., "Heterogeneous Reactor Calculation Methods" Quarterly Report No. 2, NYO-2674 September 30, 1959

3. Klahr, C. N., "Heterogeneous Reactor Calculation Methods" Quarterly Progress Report No. 1, NYO-2673, June 30, 1959, Section 2.3

4. Reference 3, Section 4

5. Feinberg, S. M., "Heterogeneous Methods for Calculating Reactors" 1955 Geneva Conference Proceedings, Vol. 5, Page 490 et. seq.

6. Arnold, W. H., and French, R. J., "Effect of U^{235} Resonance Fissions on Reactivity and Lifetime Calculations" WCAP-5243, July 31, 1958

7. Ibid.

8. Reference 3, Section 2.3

9. Reference 1

10. Reference 3 Section 4.2. One can show that the best value to take for the parameter λ is unity.

11. Kouts, H. et al., "Physics of H_2O Enriched Lattices", 1958 Geneva Conference Proceedings, Vol. 12

12. Kavanagh, D. L., "Uranium 235 Cross Sections for a Breit-Wigner Analysis", Nuclear Science and Engineering 4 155-165 (1958)

13. Reference 3, Equation (4.5b)

14. Weinberg and Wigner "The Physical Theory of Neutron Chain Reactors" University of Chicago Press (1958) Page 660 et. seq.